J Neuropathol Exp Neurol
Vol. 74, No. 3
March 2015
pp. 250–260

ORIGINAL ARTICLE

The Pathogenesis of 3 Neurotropic Flaviviruses in a Mouse Model Depends on the Route of Neuroinvasion After Viremia

Noriyo Nagata, DVM, PhD, Naoko Iwata-Yoshikawa, DVM, PhD, Daisuke Hayasaka, DVM, PhD, Yuko Sato, MT, Asato Kojima, PhD, Hiroaki Kariwa, DVM, PhD, Ikuo Takashima, DVM, PhD, Tomohiko Takasaki, MD, PhD, Ichiro Kurane, MD, PhD, Tetsutaro Sata, MD, PhD, and Hideki Hasegawa, MD, PhD

Abstract

Neurotropic flavivirus infection of humans results in viremia subsequently; in some cases, it causes meningitis encephalomyelitis, although the pathways from viremia to central nervous system (CNS) invasion are uncertain. Here, we intravenously infected BALB/c mice with 3 neurotropic flaviviruses, then examined the clinical manifestations and histopathologic changes. The Sofjin strain of tick-borne encephalitis virus–infected mice exhibited dose-dependent survival. The animals showed distention of the small intestine caused by peripheral neuritis because of infection of the myenteric plexus. Histopathologically, the strongly neurotropic Sofjin strain invaded the CNS of viremic mice via the autonomic nerves running from the plexus. The JaTH-160 strain of Japanese encephalitis virus was isolated from the lymph nodes during the preclinical phase of viral encephalitis. Therefore, this strain might infect the CNS via a hematogenous pathway, including through lymphoid tissues. The NY99-6922 strain of the West Nile virus caused clinical signs suggestive of intestinal, lymphoid, and/or neurologic involvement; the infected mice had prolonged viremia, suggesting that NY99-6922 may mainly use the hematogenous pathway; however, there was also histopathologic evidence of involvement of the autonomic nervous system pathway. In conclusion, the three neurotropic flaviviruses showed different pathogenesis, which were dependent upon overlapping but distinct pathways to CNS invasion after viremia.

Key Words: Encephalitis, Flavivirus, Japanese encephalitis virus, Mouse model, Peripheral neuritis, Tick-borne encephalitis virus, Viremia, West Nile virus.

INTRODUCTION

Tick-borne encephalitis virus (TBEV), Japanese encephalitis virus (JEV), and West Nile virus (WNV), which belong to the genus *Flavivirus* within the family *Flaviviridae*, have strong neurotropic, neuroinvasive, and neurovirulent properties. Tick-borne encephalitis virus, JEV, and WNV infections are common worldwide: TBEV infection is endemic to Western Europe, Asia, and Japan; JEV infection is prevalent in eastern and southern Asia; and there have been recent outbreaks of WNV infection in Eastern Europe, the Middle East, North America, and Australia (1).

Infection in humans, a dead-end host, occurs after a bite from an infected tick (TBEV) or mosquito (JEV and WNV); the majority of infections are either asymptomatic or symptomatic with a febrile illness. In severe cases, the neurotropic flaviviruses infect the central nervous system (CNS), resulting in viral meningitis or encephalomyelitis characterized by neuronal damage and perivascular inflammation. It is difficult to distinguish between the pathologic changes induced by these 3 neurotropic flavivirus encephalitis viruses, which preferentially target the large neurons in the human CNS (2–5). Previous studies have shown that JEV, TBEV, and WNV use common cell-surface receptors (6, 7). For example, glycosaminoglycans such as heparan sulfate proteoglycans exposed on cells within tissues, including pyramidal neurons (8), mediate flavivirus entry and infection (9). These neurotropic flaviviruses cause viremia and invade the CNS at least in part via hematogenous spread (10–12). However, the pathways from systemic infection to CNS invasion after viremia are uncertain (13, 14).

We previously examined the histopathologic features of the CNS in C57BL/6 mice subcutaneously inoculated with a neurovirulent strain of TBEV and found that the viral load in the cerebellum was significantly higher than that at other CNS sites (15, 16). Marked inflammatory cell infiltration mainly occurred in the cerebellum, meninges, and cortex, coupled with the degeneration of Purkinje cells. However, when we analyzed mice after intracerebral inoculation with TBEV, there was no difference in the histopathologic changes observed in the cerebrum and cerebellum (17). On the other hand, histopathologic examination of C57BL/6 mice subcutaneously inoculated with a neurovirulent strain of JEV revealed the main site of virus infection and inflammation to be

From the Departments of Pathology (NN, NI-Y, YS, AK, TS, HH) and Virology 1 (TT, IK), National Institute of Infectious Diseases, Tokyo; Department of Virology, Institute of Tropical Medicine, GCOE Program, Leading Graduate School Program, Nagasaki University, Nagasaki (DH); and Laboratory of Public Health, Graduate School of Veterinary Medicine, Hokkaido University, Sapporo, Hokkaido (HK, IT), Japan.

Send correspondence and reprint requests to: Noriyo Nagata, DVM, PhD, National Institute of Infectious Diseases, Musashimurayama, Tokyo, Japan; E-mail: nnagata@niid.go.jp

This work was supported by Grants-in-Aid for Research on Emerging and Re-emerging Infectious Diseases from the Ministry of Health, Labour and Welfare including H25-Shinko-ippan-007 and H26-Shinkogyosei-Shitei-002.

The authors have no conflicts of interest to declare.

the cerebral cortex (18). In addition, there was no difference between TBEV and JEV in terms of their ability to infect pyramidal neurons after intracerebral inoculation into mice. Thus, we assumed that the difference in the histopathologic features observed in these mouse models must depend on the pathway from systemic infection to CNS invasion.

Therefore, to understand the pathways of neuroinvasiveness that operate after flavivirus infection better, we developed a mouse model of flavivirus infection based on neurotropic prototype strains of TBEV, JEV, and WNV. BALB/c mice have a calm temperament, which makes them an ideal strain for a model of intravenous inoculation. This Th2-prone mouse strain was as susceptible to experimental infection with flavivirus as the Th1-prone C57BL/6 black mouse strain after intracerebral or subcutaneous inoculation (19–21). Subcutaneous injection of BALB/c mice with prototype strains of WNV and JEV resulted in a mortality rate that was lower than that after intravenous inoculation; indeed, no absolute lethal dose was reached, making it impossible to perform the study under defined conditions. Therefore, we generated a viremia model of flavivirus infection by intravenously inoculating BALB/c mice with representative neurotropic prototype strains of WNV, JEV, or TBEV.

MATERIALS AND METHODS

Tick-borne encephalitis virus infection of cultured cells and mice was performed under biosafety level 3 conditions according to the guidelines for biosafety and animal experiments at the Institute of Tropical Medicine, Nagasaki University. Animal experiments using TBEV were approved by the Biosafety and the Animal Care and Use Committees at the Institute of Tropical Medicine, Nagasaki University. Infection of cultured cells and mice with JEV and WNV was conducted under biosafety level 2 (JEV) or 3 (WNV) conditions according to the guidelines for biosafety and animal experiments of the National Institute of Infectious Diseases, Japan. Animal experiments using JEV and WNV were approved by the Committee on Biosafety and by the Animal Care and Use Committee at the National Institute of Infectious Diseases.

Viruses and Cells

The strain, origin, and passage history of the flaviviruses used in this study are listed in Table 1 (along with the relevant references). A stock prototype strain of the Far-Eastern subtype of TBEV, Sofjin (accession no. 062064) (22–24), was propagated in baby hamster kidney cells, which were maintained in Eagle minimal essential medium (Sigma-Aldrich, St. Louis, MO) containing 2% fetal bovine serum ([FBS] Sigma-Aldrich). Stock prototype strains of JEV (JaTH-160 strain [25, 26]) and WNV (NY99-6922 strain [27]) were propagated in Vero E6 cells. Vero E6 cells, purchased from American Type Cell Collection (Manassas, VA), were cultured for 2 days in Eagle minimal essential medium containing 5% FBS, 50 IU/mL of penicillin G, and 50 μg/mL of streptomycin (Gibco, Grand Island, NY). Titers of the stock viruses were expressed in terms of plaque-forming units per milliliter on Vero E6 cells.

Animal Experiments

Female BALB/c mice were purchased from Japan SLC (Shizuoka, Japan) and maintained in specific pathogen–free facilities. Mice were maintained in biosafety level 2 (for JEV) or 3 (for TBEV and WNV) animal facilities on experimental infection. The 100% lethal dose (LD_{100}) was determined by intravenous inoculation of 8-week-old adult BALB/c mice (n = 5–8 per group). Briefly, mice received 100 μL of virus solution (TBEV, 10^0–10^3 PFU/100 μL; JEV, $10^{1.8}$–$10^{4.8}$ PFU/100 μL; or WNV, $10^{3.8}$–$10^{6.8}$ PFU/100 μL) via intravenous inoculation into the tail vein and were then observed for clinical signs for 21 days thereafter. After determining the LD_{100}, 8-week-old mice (n = 10 per group) were inoculated with 1 LD_{100} of prototype strains of flavivirus, mice were observed for clinical signs, and body weights were measured once a day for 14 days postinfection (p.i.). In other experiments, 8-week-old mice were also examined at 3, 5, and 7 days p.i. and moribund animals at end point (during 6–10 days p.i.) for analysis of virus replication (n = 3 per time point) and pathology (n = 3, 9, or 14 per time point).

Virus Isolation

Animals were killed by an excess dose of isoflurane, and blood samples were obtained by cardiac puncture (TBEV, n = 3; JEV and WNV, n = 6). Tissue homogenates of brain, spinal cord, liver, spleen, kidney, lymph nodes, thymus, and Peyer patches (10% wt/vol in MEM containing 2% FBS, 50 IU of penicillin G, 50 μg of streptomycin, and 2.5 μg of amphotericin B [Gibco]) were prepared from virus-infected mice (n = 3 per time point) and clarified by centrifugation at 800 × *g* for 20 minutes. The samples were then inoculated onto Vero E6 cell cultures, which were examined for 3 days

TABLE 1. Flaviviruses Used in This Study

Virus	Strain	Origin	Passage History	Reference
Tick-borne encephalitis virus	Sofjin	Derived from a human brain infected by a Far-Eastern strain of tick-borne encephalitis virus in 1937	More than 100 passages in neonatal mouse and cultured cells	(22–24)
Japanese encephalitis virus	JaTH-160	Derived from a human case of Japanese encephalitis in 1959	Isolated after intracerebral inoculation into neonatal mouse brain, 15 passages in adult mice via intraperitoneal inoculation, and propagation in Vero cells and VeroE6 cells	(25, 26)
West Nile virus	NY99-6922	Derived from a mosquito captured in New York in 1999	Isolated by intracerebral inoculation into neonatal mouse brain and passage in C6/36 cells and Vero cells	(27)

to assess cytopathic effects. Blind passage was performed after freezing and thawing first-round passage cells. If no flavivirus-specific cytopathic effects were observed in the first- or second-round cultures, the samples were deemed negative for infectious virus.

Histopathologic and Immunohistochemical Analysis

Mice (n = 3, 9, or 14 per time point) were killed via inhalation of excess isoflurane, and the heart was perfused with 10% phosphate buffered formalin (Wako, Osaka, Japan). Brain, spinal column (including the spinal cord), lung, heart, kidney, liver, spleen, stomach, small and large intestine, thymus, and lymph node tissues were routinely processed and embedded in paraffin, sectioned, and stained with hematoxylin and eosin. The spinal column (including spinal cord) samples were decalcified in PBS (pH 7.4)/10% EDTA4Na (Dojindo, Kumamoto, Japan) before embedding. Immunohistochemical detection of TBEV, JEV, and WNV antigens was performed on paraffin-embedded sections. A rabbit polyclonal antibody against the TBEV E-protein (28), a rabbit polyclonal antibody against JEV E-protein (29), and a mouse monoclonal antibody against WNV E-protein (30, 31) were used as primary antibodies. Antigens were retrieved by 0.025% trypsin (Difco, Detroit, MI) solution containing 0.05% $CaCl_2$ (Kanto Chemical, Tokyo, Japan) for 30 minutes at 37°C (for WNV E-protein) or hydrolytic autoclaving in retrieval solution (pH 6 or pH 9; Nichirei Biosciences, Inc., Tokyo, Japan) for 10 minutes at 121°C (for TBEV E-protein and JEV E-protein). Immunohistochemical analysis was then performed using the Vector M.O.M. immunodetection Kit (Vector Laboratories, Burlingame, CA) or Nichirei-Histofine Simple Stain Mouse MAX PO (R) polymer–based detection system (Nichirei Biosciences). Peroxidase activity was detected by diaminobenzidine (Sigma-Aldrich)/hydrogen peroxide (Wako). Nuclei were counterstained with hematoxylin.

Double-Immunofluorescence Staining

To characterize the virus-infected cells, paraffin-embedded tissues were subjected to double-immunofluorescence staining with rabbit antiserum against TBEV E-protein and a chicken polyclonal antibody against the neuronal marker microtubule-associated protein 2 (MAP-2) (ab5392, Abcam, Cambridge, UK). Sections were washed 3 times with PBS (pH 7.0; Wako) after each step. Antigens were retrieved by autoclaving in retrieval solution (pH 9.0; Nichirei) at 121°C for 10 minutes. Sections were incubated with the primary rabbit polyclonal antibody against TBEV, followed by incubation with the chicken polyclonal anti–MAP-2 antibody. Sections were incubated with each primary antibody overnight at 4°C. Bound antibodies were detected using goat anti-rabbit Alexa Fluor 586 (Molecular Probes, Eugene, OR) and goat anti-chicken Alexa Fluor 488 (Molecular Probes), respectively, for 30 minutes at 37°C before mounting in SlowFade Gold antifade reagent containing 4′,6-diamidino-2-phenylindole (Molecular Probes). Images were captured under a fluorescence microscope (IX71; Olympus, Tokyo, Japan) equipped with a Hamamatsu high-resolution digital B/W CCD camera (ORCA2; Hamamatsu Photonics, Hamamatsu, Japan).

RESULTS

Viremia Model of Flavivirus Infection in BALB/c Mice

To establish a viremia model of flavivirus infection, BALB/c mice were inoculated intravenously with several different doses of the prototype strains of TBEV (Sofjin strain), JEV (JaTH-160 strain), or WNV (NY99-6922) and observed for clinical signs. The LD_{100} values for each virus were as follows: TBEV, 10^3 PFU/100 μL; JEV, $10^{2.8}$ PFU/100 μL; and WNV, 10^6 PFU/100 μL (Fig. 1A–C). A characteristic dose–response curve was observed for TBEV-infected animals but not for JEV- or WNV-infected animals. When we inoculated mice subcutaneously with JEV or WNV, we were unable to determine the LD_{100} because mice were much less susceptible to infection via this route (data not shown).

At 5 to 14 days p.i., mice intravenously inoculated with TBEV suffered weight loss and exhibited fur ruffling, a hunchback posture, and abdominal enlargement before becoming moribund (Fig. 1D). The abdominal swelling was caused by distention of the small intestine (Fig. 1E). Japanese encephalitis virus–infected BALB/c mice exhibited fur ruffling and a hunchback posture at 9 to 14 days p.i., suggesting encephalitis (Fig. 1F). At 4 to 8 days p.i., approximately 70% of WNV-infected animals exhibited fur ruffing either with or without abdominal swelling caused by distention of the small intestine (which contained black stools) (Fig. 1G, H), whereas others showed flaccid paralysis without abdominal distention (Fig. 1I).

Viral Kinetics After Intravenous Inoculation

To examine viral kinetics in the mice, we isolated the virus from blood samples (n = 3 or 6) and major organs, including the lymphatic system (n = 3), at several time points after intravenous inoculation with $1LD_{100}$ of TBEV, JEV, or WNV (Table 2). Neither TBEV nor JEV was isolated from blood samples, but WNV was isolated from both whole-blood (50% of inoculated animals) and plasma (67% of inoculated animals) samples taken on Day 3 p.i. Tick-borne encephalitis virus was isolated from the intestine, intestinal lymph nodes, and thymus on Days 3 and/or 5 p.i. Tick-borne encephalitis virus was also isolated from the brains of all infected animals during the early phase of infection (Day 5 p.i.), whereas JEV and WNV were isolated at later time points (Day 7 or 10 p.i.). Infectious JEV was isolated from the lymphatic system (spleen and lymph nodes) during the early phase of infection (Days 3 and 5 p.i.) but not on Day 7 p.i. West Nile virus was isolated from the lymphatic organs of infected mice on Days 3, 5, and 7 p.i.

Pathologic Examination of BALB/c Mice After Flavivirus Infection

We next performed pathologic examination of BALB/c mice on Days 3, 5, and 7 (n = 3 per group) and at the experimental end point (n = 3–14 per group) after intravenous inoculation with $1LD_{100}$ of TBEV, JEV, or WNV (Table 3). During the preclinical phase (within 5–7 days p.i.), no obvious histopathologic changes (e.g. inflammatory cell infiltration) were observed in any of the organs examined; however,

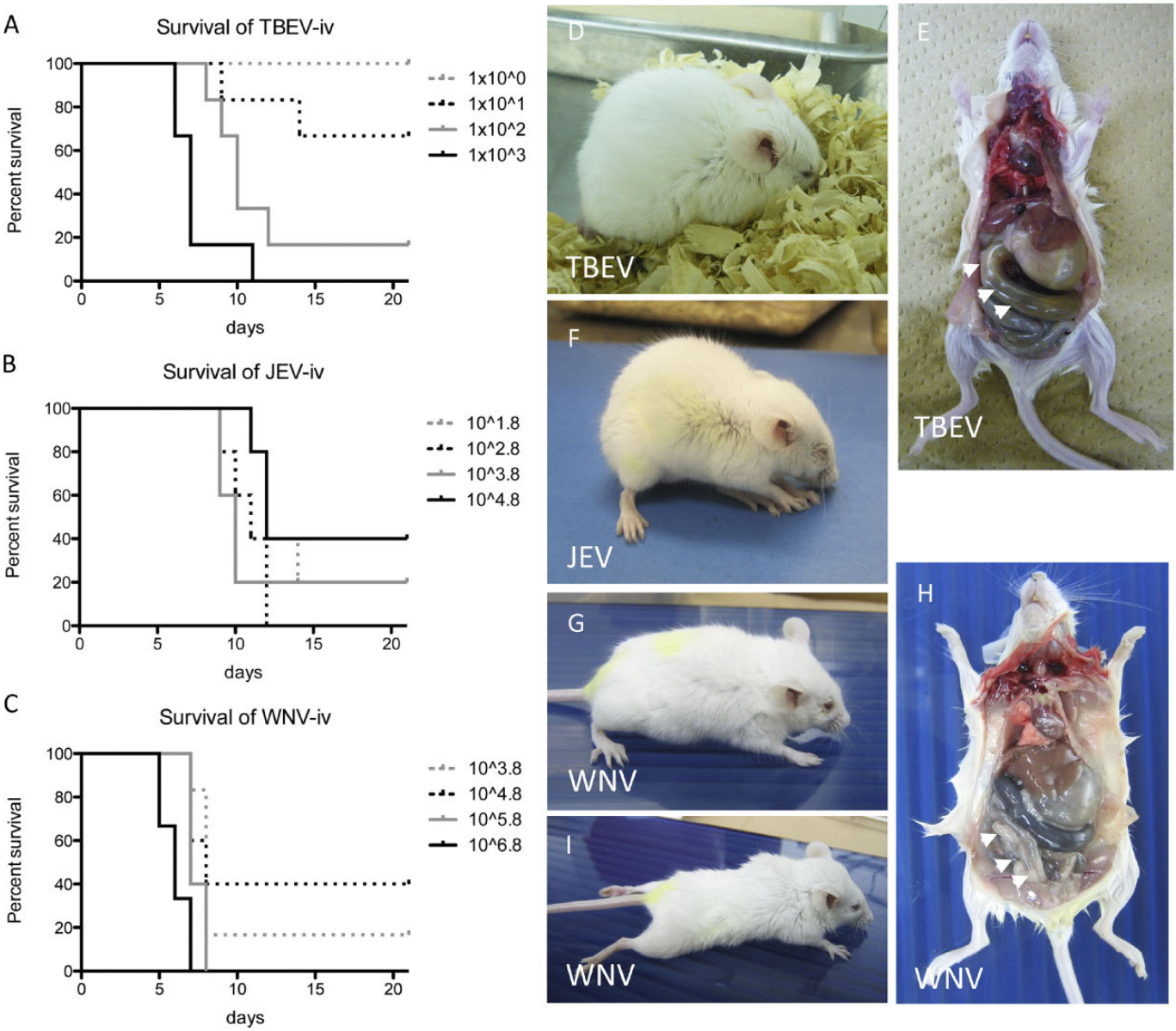

FIGURE 1. Viremia model of neurotropic flavivirus infection in BALB/c mice. **(A–C)** Survival curve showing the effect of different doses of tick-borne encephalitis virus (TBEV) **(A)**, Japanese encephalitis virus (JEV) **(B)**, and West Nile virus (WNV) **(C)** (n = 5–8 mice per group). In mice inoculated intravenously with 10^0 to 10^3 PFU of TBEV (Sofjin strain), a dose–response curve was observed **(A)**. In mice inoculated intravenously with $10^{1.8}$ to $10^{4.8}$ PFU of JEV (JaTH-160 strain), no characteristic dose–response curve was observed **(B)**. In mice inoculated with $10^{3.8}$ to $10^{6.8}$ PFU of WNV (NY99-6922), no characteristic dose–response curve was observed. **(D–I)** Mice experimentally infected with neurotropic flaviviruses seemed moribund. A TBEV-infected mouse shows fur ruffling, a hunchback posture, lack of movement, and abdominal distention **(D)**. Examination of the internal organs of a moribund TBEV-inoculated mouse demonstrates that the stomach is distended, and the small intestine is atonic and dilated (arrowheads) **(E)**. A JEV-infected mouse shows fur ruffling, a hunchback posture, and a lack of movement **(F)**. A WNV-infected mouse shows fur ruffing and abdominal distention **(G)**. Internal organs of the mouse shown in **(G)** show that the stomach is distended and the small intestine is atonic and dilated **(H)**. The contents of the small intestine were black (arrow heads). Another WNV-infected mouse showed flaccid paralysis of the hindlimbs (**I**).

1 of 3 TBEV-infected animals tested positive for viral antigens in the enteric plexus during this phase (Table 3). Tick-borne encephalitis virus antigen–positive cells were observed in the gastric plexus and enteric plexus of all animals on Day 7 p.i. On Day 8 p.i., we observed degenerated cells and an inflammatory infiltrate in the gastric plexus and enteric plexus of the TBEV-infected animals (n = 3) (Fig. 2A). Tick-borne encephalitis virus infection was observed in the celiac plexus on Day 8 p.i. (Fig. 2B), and there was abdominal distension. The lumbar spinal cord and brainstem (mainly the

TABLE 2. Virus Isolation From BALB/c Mice Intravenously Inoculated With Neuroinvasive Flaviviruses

		Virus									
		Tick-Borne Encephalitis Virus			Japanese Encephalitis Virus				West Nile Virus		
Days after inoculation‡		3 d	5 d	7 d	3 d	5 d	7 d	10 d	3 d	5 d	7 d
Blood		0*	0	0	0†	0†	0†	0†	3†	1†	1†
Plasma		NE	NE	NE	0†	0†	0†	0†	4†	0†	1†
Brain		1	3	3	0	0	2	3	1	0	1
Spinal cord		0	1	3	0	0	1	2	1	0	2
Liver		0	0	0	0	0	0	0	0	0	0
Kidney		0	0	0	0	0	0	0	0	2	1
Spleen		2	0	2	1	0	0	0	3	2	1
Lymph node	Cervical	0	0	0	1	1	0	0	3	3	3
	Axillary	0	0	0	1	1	0	2	3	3	0
	Inguinal	0	0	0	2	0	0	0	3	3	1
	Intestinal	0	3	2	0	1	0	0	1	2	1
Thymus		2	3	0	0	0	0	0	3	3	0
Intestine		2	2	1	NE	NE	0	0	1	1	2

*Number of positive animals from which virus was isolated by blind passage.
†n = 6; ‡n = 3; d, days; NE, not examined.

medulla and midbrain) from one of the TBEV-infected mice contained viral antigen–positive cells and showed a mild inflammatory reaction on each of Days 7 and 8 p.i. (Table 3; Fig. 3, left panels). Another TBEV-infected mouse showed acute neuronal degeneration, and the cerebral cortex and brainstem were positive for TBEV antigens at Day 8 p.i. (Table 3). Large neurons in the brain (in the thalamus, hypothalamus, midbrain, cerebellum, medulla, and/or cerebral cortex) and spinal cord were TVEV antigen positive (Fig. 3, left panels, insets). Lymphophagocytosis was observed in Peyer patches and other parts of the lymphoid system on Day 8 p.i., although no viral antigens were detected.

At 7 days post–JEV inoculation (preclinical phase), only 1 of 3 animals showed evidence of viral antigen–positive cells in the cerebral cortex, hippocampus, and hypothalamus (Table 3). Nine JEV-infected animals showed neurologic manifestations and became moribund on Day 9 or 10 p.i. These moribund animals had acute neuron necrosis with mild inflammation, including in the cerebral cortex, brainstem, and spinal cord (Table 3; Fig. 3, middle panels). Large neurons in the brain

TABLE 3. Histopathologic and Immunohistochemical Analysis of BALB/c Mice After Intravenous Inoculation With Flaviviruses

	Virus											
	Tick-Borne Encephalitis Virus (n = 3)				Japanese Encephalitis Virus (n = 3 or 9‡)				West Nile Virus (n = 3 or 14§)			
Day after inoculation	3 d	5 d	7 d	8 d†	3 d	5 d	7 d	9–10 d‡	3 d	5 d	7 d	6–14 d§
Myenteric plexus	0/0	1/0	3/1	3/3	0/0	0/0	0/0	0/0	0/0	0/0	0/0	0/1
Gastrointestinal tract	0/0	0/0	0/0	0/1	0/0	0/0	0/0	0/0	0/0	0/0	0/0	0/10
Brain cortex	0/0*	0/0	0/0	1/1	0/0	0/0	1/1	9/9	0/0	0/0	0/0	6/6
Hippocampus	0/0	0/0	0/0	1/1	0/0	0/0	1/0	8/8	0/0	0/0	0/0	3/4
Thalamus	0/0	0/0	1/0	2/1	0/0	0/0	0/0	9/9	0/0	0/0	0/0	6/7
Hypothalamus	0/0	0/0	1/0	2/1	0/0	0/0	1/1	4/5	0/0	0/0	0/0	3/4
Midbrain	0/0	0/0	2/0	2/1	0/0	0/0	0/0	9/9	0/0	0/0	0/0	2/3
Cerebellum	0/0	0/0	0/0	2/1	0/0	0/0	0/0	4/0	0/0	0/0	0/0	0/1
Medulla	0/0	0/0	2/0	2/1	0/0	0/0	0/0	8/9	0/0	0/0	0/0	4/3
Spinal cord	0/0	0/0	2/1	2/1	0/0	0/0	0/0	8/8	0/0	0/0	0/0	1/2
Spleen	0/0	0/0	0/0	0/2	0/0	0/0	0/0	0/2	0/0	0/0	0/0	0/11
Thymus	0/0	0/0	0/0	0/2	0/0	0/0	0/0	0/3	0/0	0/0	0/0	0/6
Cervical lymph nodes	0/0	0/0	0/0	0/2	0/0	0/0	0/0	0/2	0/0	0/0	0/0	0/6
Peyer patches	0/0	0/0	0/0	0/3	0/0	0/0	0/0	0/1	0/0	0/0	0/0	0/8

*Number of virus antigen–positive animals per number of positive animals showing histopathologic changes.
†Number of affected animals on Day 8 p.i. (n = 3).
‡Number of affected animals on Day 9 or 10 p.i. (n = 9).
§Affected animals on Days 6 to 14 (n = 14). The numbers of moribund mice on each day were Day 6, n = 3; Day 7, n = 4; Day 8, n = 3; Day 9, n = 3; and Day 14, n = 1.
d, days; p.i., postinfection.

and spinal cord were positive for viral antigens (Fig. 3, middle panels, insets). No viral antigen–positive cells or inflammatory reactions were observed in the gastrointestinal tract or celiac plexus of JEV-infected animals (Table 3; Fig. 2A, C). Lymphophagocytosis was observed in the thymus and other parts of the lymphoid system in a few moribund animals, but no viral antigens were detected.

No histopathologic lesions were observed in any of the animals during the preclinical phase post–WNV inoculation (Days 3, 5, and 7 p.i.; Table 3). Fourteen affected animals from 3 separate experiments were investigated. Overall, 10 mice showed gastrointestinal lesions; we observed neuritis of the small intestine (n = 1; Fig. 2D) and mucus hypersecretion from necrotic intestinal tissues (n = 10; Fig. 2E) and/or erosion of the large intestine (n = 2; Fig. 2F). No viral antigens were detected in the gastrointestinal lesions by immunohistochemistry (Fig. 2A, D). Seven mice had lesions in the CNS related to virus infection (Fig. 3, right panels). Large neurons, mainly in the cerebral cortex, thalamus, and medulla, were positive for viral antigens (Fig. 3, right panels, insets). Eleven animals showed reduced numbers of lymphocytes in the spleen and/or thymus (Fig. 2G); no viral antigens were detected in lymphoid organs by immunohistochemistry. Only 1 mouse had plexitis in the small intestine, along with inflammation of the meninges around the spinal cord and brainstem (Figs. 2D, 3). No viral antigens were detected in the intestine. Another mouse that had erosion and massive edema in the submucosa and muscle layer of the large intestine also showed massive lymphocyte depletion in the thymic cortex; however, there were no lesions in the CNS (Fig. 2F, G).

The Sofjin Strain of TBEV Invades the CNS via a Neuronal Pathway From the Gastrointestinal Tract

Tick-borne encephalitis virus was isolated from intestinal tissues of TBEV-infected mice; the gastric myenteric plexus and celiac plexus were positive for viral antigens on Days 5 and 7 p.i. To confirm TBEV infection in the peripheral nerves of the small intestine, tissues were double stained to detect viral antigens and the neuronal marker MAP-2. Large MAP-2–positive neurons in the gastric plexus and celiac plexus were positive for viral antigens on Day 5 p.i. but not on Day 3 p.i. (Fig. 4). These data suggest that the virus infected the CNS via the gastrointestinal autonomic nerves.

DISCUSSION

The ability of a neurotropic virus to invade and establish an infection within the CNS is one of the most important factors that determine its neuropathogenicity. There are 3 main routes of entry to the CNS: the neural pathway, the olfactory route, and the hematogenous route. Evidence for neuroinvasion by way of the peripheral nervous system has been reported for rabies virus (32), alpha herpes viruses (33, 34), poliovirus (35, 36), and flavivirus (37). Here, we demonstrate that intravenous inoculation of BALB/c mice with the representative neurotropic flaviviruses TBEV, JEV, and WNV resulted in different clinical and histopathologic characteristics, which seemed to correlate with the neuroinvasive features of the viruses.

The histopathologic features of flavivirus infections in the CNS include neuron necrosis, neuronophagy, and perivascular inflammatory infiltrates. Viral antigens are also identified in large neurons within the human CNS (4, 5, 38). Here, we found that the large nerve cells in the brain and spinal cord of BALB/c mice were highly susceptible to these 3 neurotropic flaviviruses, although the inflammatory reactions were mild. Various neurologic manifestations caused by disorders of the CNS and/or peripheral nervous system, including the autonomic nervous system, have been reported in humans (38–40); however, there is no direct evidence that flaviviruses infect the autonomic nerves. Thus, the animal model described herein will increase our understanding of the pathology of neurotropic flaviviruses.

Here, we found that mice intravenously inoculated with the Sofjin strain exhibit an expected dose–response curve. Histopathologic analysis revealed that the Sofjin strain infected the nerves associated with the intestine during the preclinical phase. Sofjin is a strongly neurotropic strain of TBEV because of long-term passage in the brains of suckling mice (22–24). Animal models infected with strongly neurotropic viruses (such as transgenic mice bearing the human poliovirus receptor or mice infected with herpes simplex virus type 1) show dose–response curves after intraspinal or subcutaneous inoculation (41–43). Even experimental models of neuronal pathway infections, such as intracerebral inoculation with flavivirus, show a dose–response curve that is explained by the viral load and neurovirulence of this virus. The characteristic dose–response curve observed in TBEV-infected animals in the present study may also be the result of the viral load and the neurovirulence of the Sofjin strain; intravenous injection resulted in CNS infection via the peripheral nerves (the autonomic nerves) in the gut. Humans infected with TBEV also show gastrointestinal symptoms during the acute phase, along with progressive neuritis and neuropsychiatric sequelae. In addition, autonomic involvement, including gastrointestinal tract symptoms, orthostatic hypotension, and urinary retention, has been reported in TBE cases (39). Histopathologic examination of Sofjin-infected mice suggested that the virus infected the brainstem via the gastrointestinal peripheral nerves (i.e. the vagus nerve). Therefore, this animal model mimics human neuritis caused by TBEV infection.

On the other hand, in the present study, no dose–response curves were observed for JEV- and WNV-infected animals. This finding is similar to that reported for intraperitoneal or subcutaneous inoculation models of flavivirus infection (44, 45). Intranasal inoculation with WNV results in a more predictable dose–response curve because the virus infects the CNS via the olfactory nerves (44). Thus, it is possible that neither JEV nor WNV uses neuronal pathways in our viremia model.

Japanese encephalitis virus was rapidly cleared from the blood after inoculation and was present in the lymph node during the preclinical phase. By contrast, WNV-infected mice showed prolonged viremia. This may be because JEV replicated in macrophages and dendritic cells in peripheral organs such as the lymph nodes and spleen (46, 47). Liu et al (48) used Evans blue dye to demonstrate an increase in blood–brain

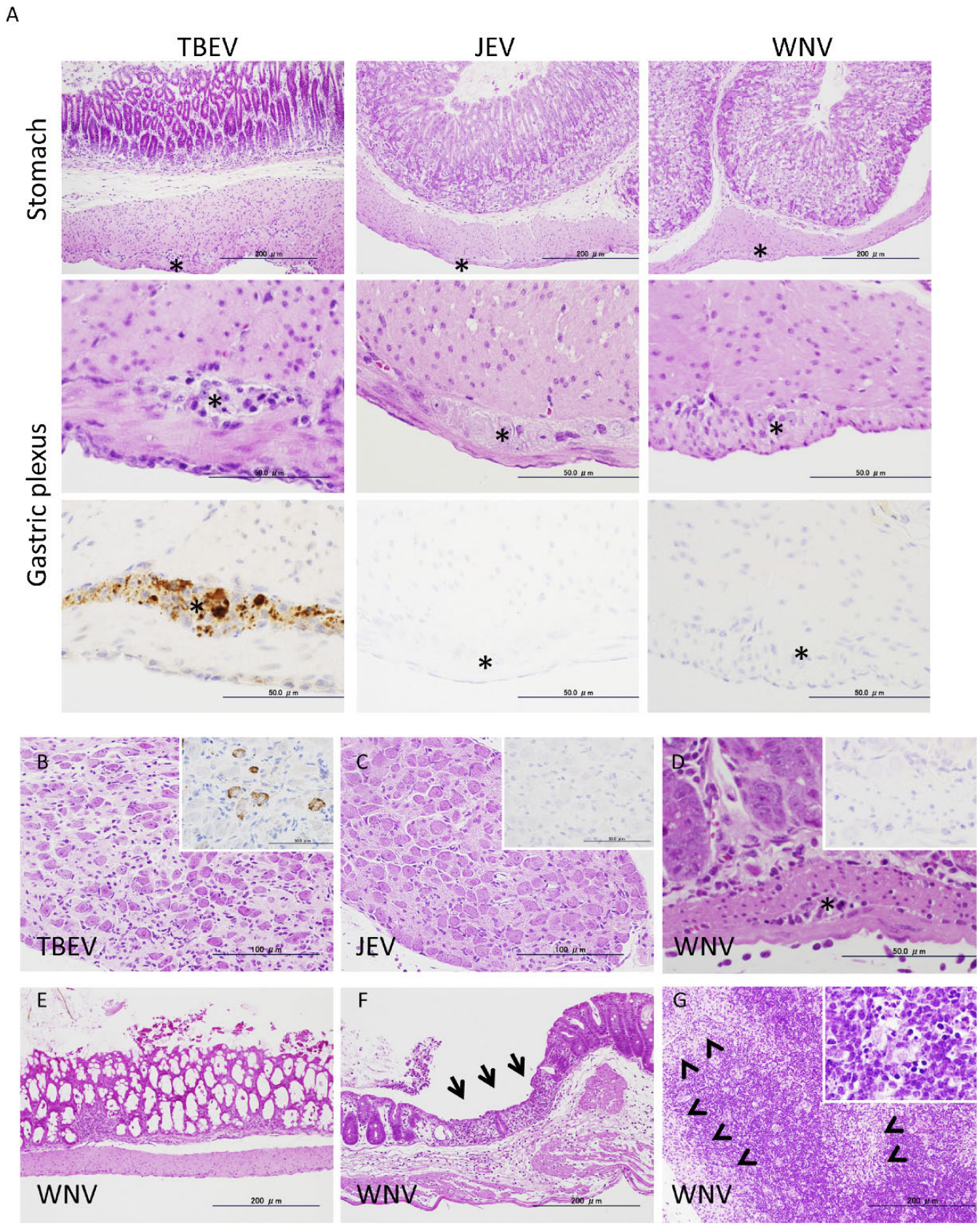

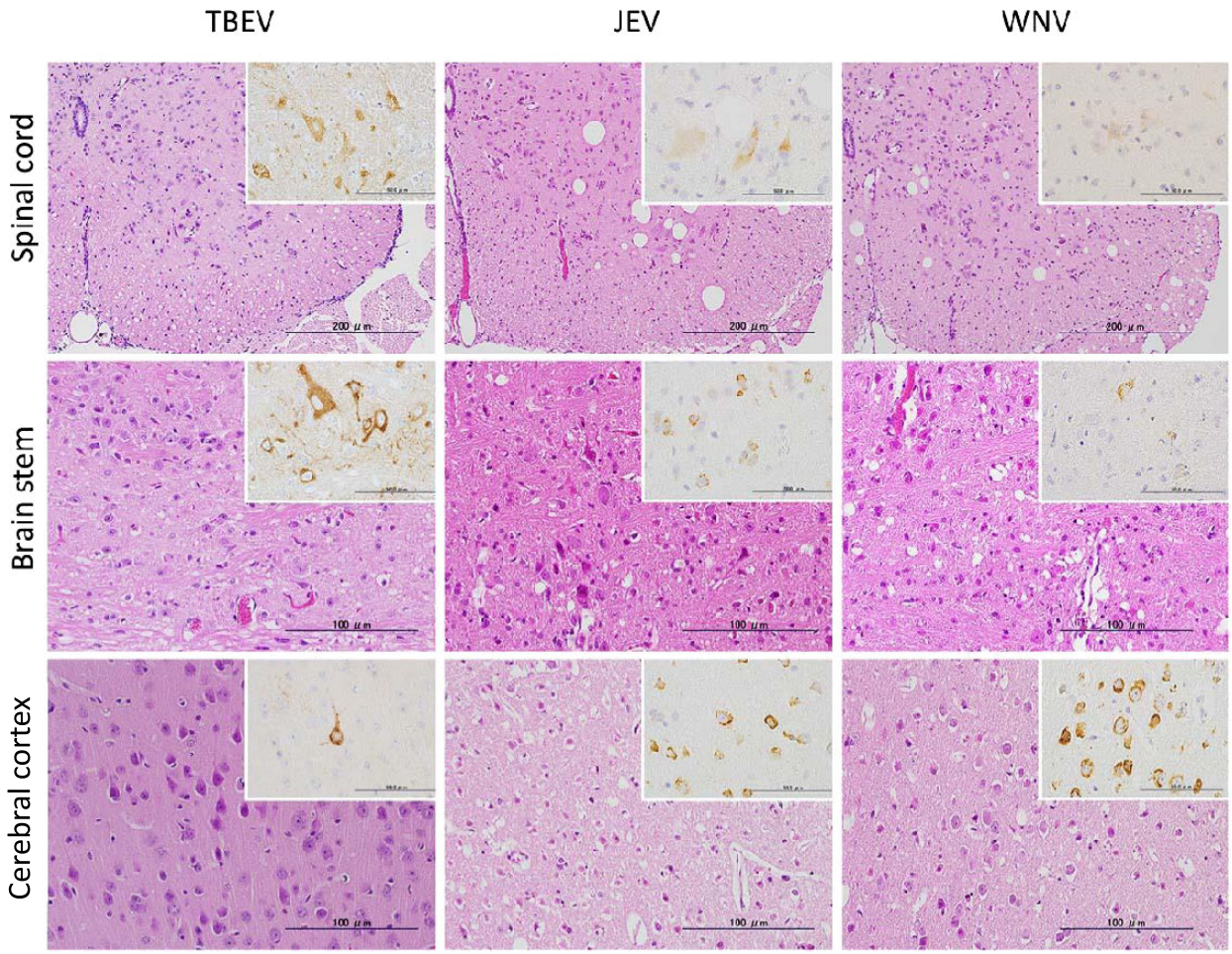

FIGURE 3. CNS lesions in neurotropic flavivirus-infected BALB/c mice. Tissues were obtained from moribund mice after intravenous inoculation with tick-borne encephalitis virus (TBEV, 10^3 PFU/100 μL of Sofjin strain) (left panels), Japanese encephalitis virus (JEV, $10^{2.8}$ PFU/100 μL of JaTH-160 strain) (middle panels), and West Nile virus (WNV, 10^6 PFU/100 μL of NY99/6922 strain) (right panels). Left column panels: Degenerated neurons with or without inflammatory infiltration in the spinal cord, medulla, and cerebral cortex of a mouse on Day 8 postinfection (p.i.) with TBEV. Immunohistochemistry (IHC, insets) revealed that the pyramidal neurons in the lesion were positive for viral antigens (middle panel). Middle column panels: Degenerated neurons in the spinal cord and medulla of a JEV-infected mouse were positive for viral antigens. Acute necrotic neurons in the cerebral cortex were strongly positive for viral antigens (inset). Right column panels: A WNV-infected mouse suffering from paralysis showed neuronophagia and mild inflammatory infiltrates in the spinal cord and medulla. Very few virus antigen–positive cells were seen in the lesions. Acute necrotic or degenerated neurons in the cerebral cortex were strongly positive for viral antigens (inset).

FIGURE 2. Histopathologic examination of the intestines and mesentery tissue from neurotropic flavivirus-infected BALB/c mice. Tissues were obtained from mice after intravenous inoculation with tick-borne encephalitis virus (TBEV Sofjin strain; 10^3 PFU/100 μL), Japanese encephalitis virus (JEV JaTH-160 strain; $10^{2.8}$ PFU/100 μL), or West Nile virus (WNV NY99/6922 strain; 10^6 PFU/100 μL). **(A)** The gastric plexus can be seen between the muscle layers of the stomach (upper and middle panels, asterisks). Inflammatory infiltrations in the gastric plexus and in the serous membrane of a TBEV-infected mouse (left of middle panel). Virus antigen–positive cells are present in the lesion in the gastric plexus of the TBEV-infected mouse (lower left panel) but not in the mice infected with JEV or WNV. **(B)** The celiac plexus within the mesentery tissue from a TBEV-infected mouse contained degenerated neurons and an inflammatory infiltrate composed of mononuclear cells. Virus antigen–positive cells were observed in the lesion (inset). **(C)** The celiac plexus within the mesenteric tissue of a JEV-infected mouse. No histopathologic changes and no viral antigens were observed. **(D)** Degenerated and necrotic cells in the intestinal plexus of the duodenum in a WNV-infected mouse. **(E)** Hypersecretion of mucin in the large intestine of a WNV-infected mouse. **(F)** Erosive and congested intestine from a moribund WNV-infected mouse. Lesion with a necrotic epithelium and an inflammatory cell infiltrate (arrows). There is massive edema, fibrin formation, and inflammation in the submucosa and muscle layer. **(G)** Lymphocyte-depleted cortex within the thymus of a WNV-infected mouse (arrowheads). There are numerous tangible macrophages in the medulla (inset). Upper and middle panels of **(A and B–G)**: H&E, hematoxylin and eosin staining. Lower panels of **(A)** and the insets in **(B–D)**: immunohistochemical analysis using anti-TBEV, JEV, or WNV antibodies.

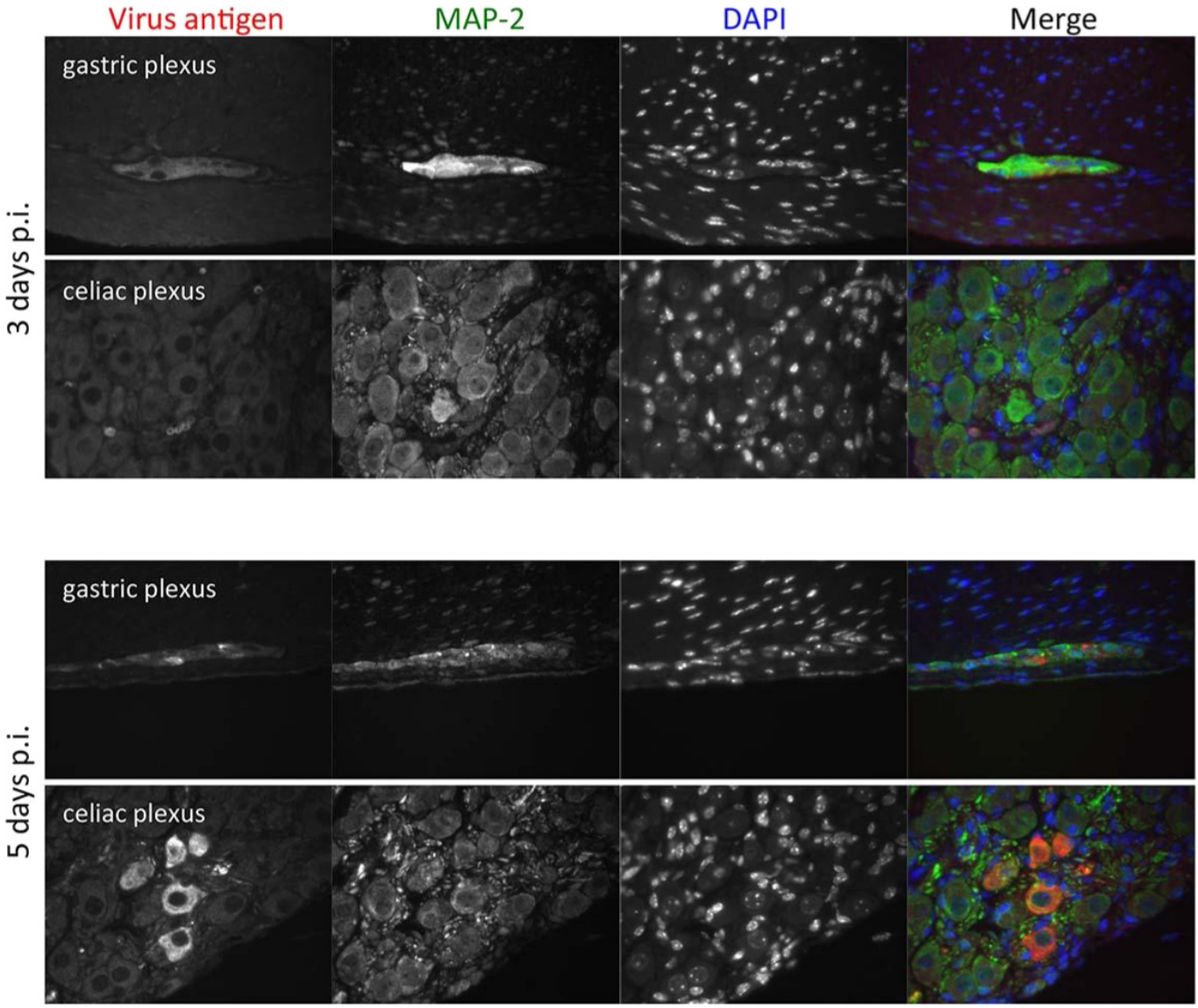

FIGURE 4. Double immunofluorescence staining detected tick-borne encephalitis virus (TBEV)–infected cells in BALB/c mice. TBEV viral antigens (red) colocalized with microtubule-associated protein 2 (MAP-2)–positive nerve cells (green) in the gastric plexus and celiac plexus on Day 5 but not on Day 3 postinfection (p.i.). DAPI, 4′,6-diamidino-2-phenylindole (blue).

barrier permeability after intravenous inoculation with JEV. This change in permeability allowed the virus and/or putatively infected leukocytes to access the cerebrum, thereby initiating CNS infection. The results of the present study may support this conclusion because histopathologic analysis of infected mice suggested that the cerebrum, hippocampus, and hypothalamus were the initial sites of JEV infection. The infection then spread throughout the brain and spinal cord. However, we found no clear evidence for the suggested mechanism of JEV spread within the CNS.

The pathology of WNV infection in this mouse model was complex. West Nile virus–infected mice showed various clinical signs and pathologic features, including neurologic, lymphoid, and intestinal disorders. Histopathologic examination suggested that the pathology observed in the mice suffering from viral encephalitis was similar to that observed in JEV-infected mice; however, the intestinal disorders seemed different from those in TBEV-infected mice. Tick-borne encephalitis virus infection of the gastrointestinal plexus was the main cause of stomach and small intestine dilatation in TBEV-infected mice. By contrast, only 1 WNV-infected mouse showed evidence of neuronal degeneration and inflammatory infiltration into the intestinal plexus; other mice had erosive enteritis and circulatory failure, with no evidence of viral infection of the intestine. Two previous mouse model studies report gastric and small intestinal distention after subcutaneous or intraperitoneal infection by WNV infection; however, the microscopic findings in these studies were different from those reported herein (49, 50). A possible reason for this discrepancy might be differences in virulence between the strains. In addition, we found that some WNV-infected mice showed marked lymphocyte depletion within the lymphoid tissues in

the absence of encephalitis and neuritis. It is possible that the intestinal erosion and thymic atrophy were caused by ''nonspecific'' stress responses after a viral infection. On the other hand, massive lymphocyte depletion, including thymic atrophy, is a common finding in moribund mice after WNV infection (49–51). Thus, the histopathologic findings suggest that the mechanism underlying CNS pathogenesis is different in individual mice. Shirato et al (52) found that the NY99-6922 stock virus produced plaques of 2 different sizes. After plaque cloning, the cloned variants showed different levels of virulence after subcutaneous inoculation into mice. Both small- and large-plaque variants infected the blood and spleen of the mice after subcutaneous inoculation, and the small-plaque variant did not infect the CNS. Intracerebral inoculation into mice revealed that these 2 variants had different neurovirulence (52). Such different variants might be 1 reason that we observed different clinical manifestations and pathologies in individual NY99-6922–infected mice.

In summary, histopathologic examination suggested that the 3 neurotropic prototype strains of flaviviruses examined herein invaded via the neuronal pathway (Sofjin strain of TBEV), the hematogenous pathway, and/or the lymphogenous pathway (JaTH strain of JEV and/or NY99 strain of WNV) after intravenous inoculation into mice. Taken together, our results suggest that the observed differences in the clinical and pathologic features of each virus depend on the pathway by which the virus invades neuronal tissues. Thus, the present study increases our understanding of the neuropathology underlying the neuroinvasiveness of these neurotropic flaviviruses.

ACKNOWLEDGMENT

The authors thank Ms. Mihoko Fujino, Moeko Aida, and Ayako Harashima for technical assistance.

REFERENCES

1. Pierson TC, Diamond MS. Flaviviruses. In: Knipe DM, Howley P, eds. *Fields Virology, Vol. 1*. Philadelphia, PA: Wolters Kluwer Health, 2013: 747–94
2. Agamanolis DP, Leslie MJ, Caveny EA, et al. Neuropathological findings in West Nile virus encephalitis: A case report. Ann Neurol 2003;54: 547–51
3. Cushing MM, Brat DJ, Mosunjac MI, et al. Fatal West Nile virus encephalitis in a renal transplant recipient. Am J Clin Pathol 2004;121: 26–31
4. Gelpi E, Preusser M, Garzuly F, et al. Visualization of Central European tick-borne encephalitis infection in fatal human cases. J Neuropathol Exp Neurol 2005;64:506–12
5. Wong KT, Ng KY, Ong KC, et al. Enterovirus 71 encephalomyelitis and Japanese encephalitis can be distinguished by topographic distribution of inflammation and specific intraneuronal detection of viral antigen and RNA. Neuropathol Appl Neurobiol 2012;38:443–53
6. Kaufmann B, Rossmann MG. Molecular mechanisms involved in the early steps of flavivirus cell entry. Microbes Infect 2011;13:1–9
7. Perera-Lecoin M, Meertens L, Carnec X, et al. Flavivirus entry receptors: An update. Viruses 2014;6:69–88
8. Litwack ED, Stipp CS, Kumbasar A, et al. Neuronal expression of glypican, a cell-surface glycosylphosphatidylinositol-anchored heparan sulfate proteoglycan, in the adult rat nervous system. J Neurosci 1994;14: 3713–24
9. Chien YJ, Chen WJ, Hsu WL, et al. Bovine lactoferrin inhibits Japanese encephalitis virus by binding to heparan sulfate and receptor for low density lipoprotein. Virology 2008;379:143–51
10. Gea-Banacloche J, Johnson RT, Bagic A, et al. West Nile virus: Pathogenesis and therapeutic options. Ann Intern Med 2004;140:545–53
11. Liu Y, Chuang CK, Chen WJ. In situ reverse-transcription loop-mediated isothermal amplification (in situ RT-LAMP) for detection of Japanese encephalitis viral RNA in host cells. J Clin Virol 2009;46:49–54
12. Schultze D, Dollenmaier G, Rohner A, et al. Benefit of detecting tick-borne encephalitis viremia in the first phase of illness. J Clin Virol 2007;38: 172–75
13. Clark DC, Brault AC, Hunsperger E. The contribution of rodent models to the pathological assessment of flaviviral infections of the central nervous system. Arch Virol 2012;157:1423–40
14. Neal JW. Flaviviruses are neurotropic, but how do they invade the CNS? J Infect 2014;69:203–15
15. Hayasaka D, Nagata N, Fujii Y, et al. Mortality following peripheral infection with tick-borne encephalitis virus results from a combination of central nervous system pathology, systemic inflammatory and stress responses. Virology 2009;390:139–50
16. Takashima I, Morita K, Chiba M, et al. A case of tick-borne encephalitis in Japan and isolation of the the virus. J Clin Microbiol 1997;35:1943–47
17. Yoshii K, Moritoh K, Nagata N, et al. Susceptibility to flavivirus-specific antiviral response of Oas1b affects the neurovirulence of the Far-Eastern subtype of tick-borne encephalitis virus. Arch Virol 2013; 158:1039–46
18. Hayasaka D, Shirai K, Aoki K, et al. TNF-alpha acts as an immunoregulator in the mouse brain by reducing the incidence of severe disease following Japanese encephalitis virus infection. PLoS One 2013;8: e71643
19. Miura K, Goto N, Suzuki H, et al. Strain difference of mouse in susceptibility to Japanese encephalitis virus infection. Jikken Dobutsu 1988; 37:365–73
20. Ruzek D, Salat J, Palus M, et al. $CD8^+$ T-cells mediate immunopathology in tick-borne encephalitis. Virology 2009;384:1–6
21. Samuel MA, Diamond MS. Pathogenesis of West Nile virus infection: A balance between virulence, innate and adaptive immunity, and viral evasion. J Virol 2006;80:9349–60
22. Chiba N, Iwasaki T, Mizutani T, et al. Pathogenicity of tick-borne encephalitis virus isolated in Hokkaido, Japan in mouse model. Vaccine 1999;17:779–87
23. Shamanin VA, Pletnev AG, Rubin SG, et al. Differentiation of strains of tick-borne encephalitis virus by means of RNA-DNA hybridization. J Gen Virol 1990;71:1505–15
24. Hayasaka D, Ivanov L, Leonova GN, et al. Distribution and characterization of tick-borne encephalitis viruses from Siberia and far-eastern Asia. J Gen Virol 2001;82:1319–28
25. Nishimura C, Nomura M, Kitaoka M. Comparative studies on the structure and properties of two selected strains of Japanese encephalitis virus. Jpn J Med Sci Biol 1968;21:1–10
26. Fujisaki Y, Miura Y, Sugimori T, et al. Experimental studies on vertical infection of mice with Japanese encephalitis virus. IV. Effect of virus strain on placental and fetal infection. Natl Inst Anim Health Q (Tokyo) 1983;23:21–26
27. Shirato K, Mizutani T, Kariwa H, et al. Discrimination of West Nile virus and Japanese encephalitis virus strains using RT-PCR RFLP analysis. Microbiol Immunol 2003;47:439–45
28. Yoshii K, Konno A, Goto A, et al. Single point mutation in tick-borne encephalitis virus prM protein induces a reduction of virus particle secretion. J Gen Virol 2004;85:3049–58
29. Kojima A, Yasuda A, Asanuma H, et al. Stable high-producer cell clone expressing virus-like particles of the Japanese encephalitis virus e protein for a second-generation subunit vaccine. J Virol 2003;77:8745–55
30. Ohtaki N, Takahashi H, Kaneko K, et al. Immunogenicity and efficacy of two types of West Nile virus-like particles different in size and maturation as a second-generation vaccine candidate. Vaccine 2010;28:6588–96
31. Ohtaki N, Takahashi H, Kaneko K, et al. Purification and concentration of non-infectious West Nile virus–like particles and infectious virions using a pseudo-affinity Cellufine Sulfate column. J Virol Methods 2011; 174:131–35
32. Gillet JP, Derer P, Tsiang H. Axonal transport of rabies virus in the central nervous system of the rat. J Neuropathol Exp Neurol 1986;45: 619–34

33. Bak IJ, Markham CH, Cook ML, et al. Ultrastructural and immunoperoxidase study of striatonigral neurons by means of retrograde axonal transport of herpes simplex virus. Brain Res 1978;143:361–68
34. Penfold ME, Armati P, Cunningham AL. Axonal transport of herpes simplex virions to epidermal cells: Evidence for a specialized mode of virus transport and assembly. Proc Natl Acad Sci U S A 1994;91:6529–33
35. Ohka S, Matsuda N, Tohyama K, et al. Receptor (CD155)-dependent endocytosis of poliovirus and retrograde axonal transport of the endosome. J Virol 2004;78:7186–98
36. Ren R, Racaniello VR. Poliovirus spreads from muscle to the central nervous system by neural pathways. J Infect Dis 1992;166:747–52
37. Samuel MA, Wang H, Siddharthan V, et al. Axonal transport mediates West Nile virus entry into the central nervous system and induces acute flaccid paralysis. Proc Natl Acad Sci USA 2007;104:17140–45
38. Hayes EB, Sejvar JJ, Zaki SR, et al. Virology, pathology, and clinical manifestations of West Nile virus disease. Emerg Infect Dis 2005;11:1174–79
39. Kleiter I, Steinbrecher A, Flugel D, et al. Autonomic involvement in tick-borne encephalitis (TBE): Report of five cases. Eur J Med Res 2006;11:261–65
40. Nash D, Mostashari F, Fine A, et al. The outbreak of West Nile virus infection in the New York City area in 1999. N Engl J Med 2001;344:1807–14
41. Abe S, Ota Y, Doi Y, et al. Studies on neurovirulence in poliovirus-sensitive transgenic mice and cynomolgus monkeys for the different temperature-sensitive viruses derived from the Sabin type 3 virus. Virology 1995;210:160–66
42. Dix RD, McKendall RR, Baringer JR. Comparative neurovirulence of herpes simplex virus type 1 strains after peripheral or intracerebral inoculation of BALB/c mice. Infect Immun 1983;40:103–12
43. Horie H, Koike S, Kurata T, et al. Transgenic mice carrying the human poliovirus receptor: New animal models for study of poliovirus neurovirulence. J Virol 1994;68:681–88
44. King NJ, Getts DR, Getts MT, et al. Immunopathology of flavivirus infections. Immunol Cell Biol 2007;85:33–42
45. Shrestha B, Wang T, Samuel MA, et al. Gamma interferon plays a crucial early antiviral role in protection against West Nile virus infection. J Virol 2006;80:5338–48
46. Aleyas AG, George JA, Han YW, et al. Functional modulation of dendritic cells and macrophages by Japanese encephalitis virus through MyD88 adaptor molecule–dependent and –independent pathways. J Immunol 2009;183:2462–74
47. Kurane I. Immune responses to Japanese encephalitis virus. Curr Top Microbiol Immunol 2002;267:91–103
48. Liu TH, Liang LC, Wang CC, et al. The blood–brain barrier in the cerebrum is the initial site for the Japanese encephalitis virus entering the central nervous system. J Neurovirol 2008;14:514–21
49. Kimura T, Sasaki M, Okumura M, et al. Flavivirus encephalitis: Pathological aspects of mouse and other animal models. Vet Pathol 2010;47:806–18
50. Williams JH, Mentoor JD, Van Wilpe E, et al. Comparative pathology of neurovirulent lineage 1 (NY99/385) and lineage 2 (SPU93/01) West Nile virus infections in BALBc mice. Vet Pathol 2014;52:140–151
51. Garcia-Tapia D, Hassett DE, Mitchell WJ Jr, et al. West Nile virus encephalitis: Sequential histopathological and immunological events in a murine model of infection. J Neurovirol 2007;13:130–38
52. Shirato K, Miyoshi H, Goto A, et al. Viral envelope protein glycosylation is a molecular determinant of the neuroinvasiveness of the New York strain of West Nile virus. J Gen Virol 2004;85:3637–45